Advances in Nano Research, *Vol. 15, No. 2 (2023) 165-174*
https://doi.org/10.12989/anr.2023.15.2.165

Analyzing the mechano-bactericidal effect of nano-patterned surfaces by finite element method and verification with artificial neural networks

Ecren Uzun Yaylacı*[1], Murat Yaylacı[2,3], Mehmet Emin Özdemir[4], Merve Terzi[5], Şevval Öztürk[2]

[1]*Faculty of Engineering and Architecture, Recep Tayyip Erdogan University, 53100, Rize, Turkey*
[2]*Department of Civil Engineering, Recep Tayyip Erdogan University, 53100, Rize, Turkey*
[3]*Biomedical Engineering MSc Program, Recep Tayyip Erdogan University, 53100, Rize, Turkey*
[4]*Department of Civil Engineering, Cankiri Karatekin University, 18100, Çankırı, Turkey*
[5]*Department of Civil Engineering, Istanbul Rumeli University, 34570, Istanbul, Turkey*

(*Received February 24, 2023, Revised June 4, 2023, Accepted June 8, 2023*)

Abstract. The study investigated the effect of geometric structures of nano-patterned surfaces, such as peak sharpness, height, width, aspect ratio, and spacing, on mechano-bactericidal properties. Here, in silico models were developed to explain surface interactions with *Escherichia coli*. Numerical solutions were performed based on the finite element method and verified by the artificial neural network method. An *E. coli* cell adhered to the nano surface formed elastic and creep deformation models, and the cells' maximum deformation, maximum stress, and maximum strain were calculated. The results determined that the increase in peak sharpness, aspect ratio, and spacing values increased the maximum deformation, maximum stress, and maximum strain on *E. coli* cell. In addition, the results showed that FEM and ANN methods were in good agreement with each other. This study proved that the geometrical structures of nano-patterned surfaces have an important role in the mechano-bactericidal effect.
Keywords: artificial neural network; finite element method; mechano-bactericidal; nano-patterned surface

1. Introduction

The biofilm layer formed after bacterial colonization on the surfaces is one of the main factors that initiate the infection. Treatments based on antibiotics or containing various chemicals are used in bacterial infections. However, toxicity and increasing antibiotic-resistant strains pose a severe problem regarding public health, the environment, and food safety (Meek *et al*. 2015, Uzun Yaylacı 2021). Therefore, sustainable, safe, and environmentally friendly methods are needed to reduce these risk factors. In recent years, an innovative and alternative mechano-bactericidal approach has been developed, inspired by the prevention of bacterial colonization and biofilm formation by naturally structured nanosurfaces (Cui *et al*. 2021, Alameda *et al*. 2022). It has been discovered that lotus leaves (Green et *al*. 2017), gecko skin (Hazell *et al*. 2018), and wings of various insects (Cao *et al*. 2018, Jiang *et al*. 2020) have nano-structures that can inhibit bacterial adhesion/growth in nature. Inspired by the bactericidal properties of structures on natural surfaces, synthetic nano-pattern surfaces that mimic this mechanical biocidal mechanism have been fabricated (Bagherifard *et al*. 2015, Maleki *et al*. 2021).

Mechano-bactericidal activity is affected by many factors, such as aspect ratio, shape, spacing, and contact area of nanostructures on the surface (Zhou *et al*. 2021). In addition, some bacterial strain characteristics, including intrinsic factors, cell wall structure, and size, are also effective in bactericidal activity (Linklater *et al*. 2017). In the analysis evaluating the mechano-bactericidal effects of nanostructures, it is accepted that the physical rupture of the cell wall causes the leakage of the cytoplasm of the bacteria and eventually leads to its death (Pogodin *et al*. 2013, Roy and Chatterjee 2021). There is a consensus that the bactericidal effect of such nanosurfaces is the result of mechanical forces (Ivanova *et al*. 2012, 2020). The interaction of bacteria with nanostructures is a dynamic process influenced by many factors. The effect of each factor on the bactericidal performance of the surface and the most effective mechano-bactericidal mechanism has yet to be fully understood. Most of the uncertainties arise from the difficulty of characterizing the interaction process of bacteria and nanostructures (Alameda *et al*. 2022). For this reason, computer-aided numerical simulations, in which many factors can be analyzed simultaneously, are widely used to eliminate uncertainties.

Many different methods are used to solve engineering problems (Hadji and DarAssi 2014, DarAssi and Hadji 2014, DarAssi 2021, Sun *et al*. 2022, Noori *et al*. 2022, Abharian *et al*. 2023, Fu *et al*. 2023). The finite element method (FEM) is an analysis used in engineering to solve differential equations through mathematical modeling. Contact and crack mechanics solutions are among the uses of FEM (Pandey *et al*. 2019, Kumar *et al*. 2021, Bouafia *et al*. 2021, Yaylacı *et al*. 2021, 2022a). However, only a few studies have used finite element analysis to simulate *in-silico* interactions between bacteria and nano-patterned surfaces (Mirzaali *et al*. 2018, Velic *et al*. 2021, Cui *et al*.

*Corresponding author, Ph.D., Associate Professor,
E-mail: ecren.uzunyaylaci@erdogan.edu.tr

Copyright © 2023 Techno-Press, Ltd.

ISSN: 2287-237X (Print), 2287-2388 (Online)

2021). Although it is known that the geometric structure of nano-patterned surfaces influences bactericidal properties, the effects of basic geometric parameters are still not fully understood.

This study aimed to simulate the mechano-bactericidal effect of the geometric parameters of nano-patterned surfaces (peak sharpness, height, width, aspect ratio, and spacing) on *Escherichia coli*. Cell-surface interactions were calculated with numerical solutions based on FEM methods, and the results were validated with the artificial neural network (ANN). For this purpose, elastic and creep deformation models of an *E. coli* cell adhered to the nano-surface were created, and cell deformation, stress, and strain were calculated.

2. Materials and methods

2.1 Finite element model and bacterial cell

In this study, a finite element model representing a three-dimensional thin wall with turgor pressure was designed using the finite element software ANSYS Workbench package program (ANSYS 2013). This module can analyze the kinetic reaction of the material under various mechanical stresses and strains (Eltaher *et al*. 2019, Yaylacı 2022, Yaylacı *et al*. 2022b, Özdemir and Yaylacı 2023). The FEM analyses help to identify a role played in the determination of optimal bacterial effects by geometrical features, and the aim was to simulate the interactions between each bacteria species and the nanoparticles. Gram-negative and rod-shaped *E. coli* was used as a model bacterium to investigate cell-surface interaction. An *E. coli* cell is approximately 2 μm length and 0.5 μm in diameter (Vadillo-Rodriguez *et al*. 2009) with a cell wall thickness of 6 nm (Turner *et al*. 2013). Figure 1 shows the schematic illustration of the cell dimensions and wall of *E. coli.*

The height, width, and spacing are basic geometrical parameters for the nano-patterns exhibited in Figure 2. In the analyses, the nano-patterns geometric property is taken as height=200 nm. Other parameters are chosen such as width, peak, and spacing which are compatible with solutions. Peak sharpness is categorized into five groups including flat (0), ellipse (0.25), quasi-flat (0.5), semi-circular (0.75), and sharp tip shapes (1.0).

The presence of the bacterial cytoplasm and turgor pressure was indicated by the application of uniform pressure within the cell wall. The turgor pressure of an *E. coli* cell is 0.03 MPa. Therefore, bacteria were simulated by applying a uniform pressure of 0.03 MPa on the inner wall of the cell. Subsequently, interactions between the cells and the nanopillar surfaces were also simulated. The adherence of the *E. coli* cell is achieved using a vertical load on the entire cell surface. During this process, the cell's turgor pressure remained stable. The cell-surface interaction is modeled on a contact surface-to-surface with a normal contact behavior with the penalty formulation based on the coefficient of friction $\mu = 2$ (Cui *et al*. 2021).

The elastic properties of *E. coli* cell wall are used Young's modulus and Poisson's ratio as 25 MPa and 0.16,

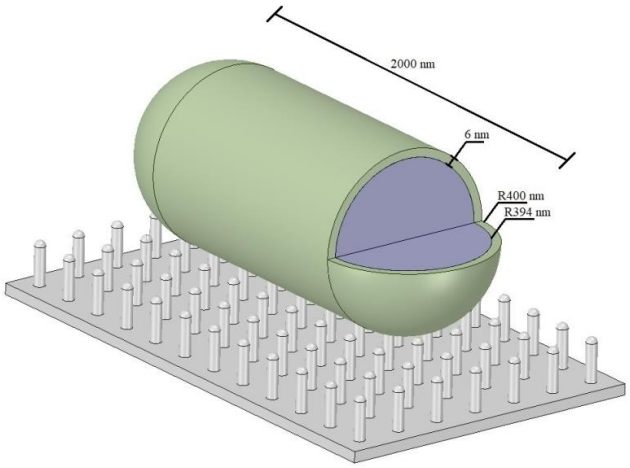

Fig. 1 The schematic illustration of the cell dimensions and wall of *E. coli*

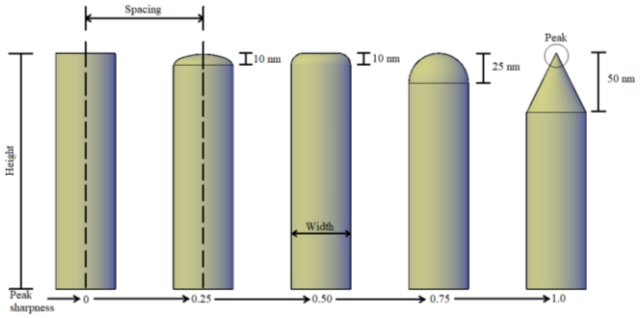

Fig. 2 The schematic illustration of the nano-patterns

Table 1 Optimum values of concentration and drug fraction for minimizing, maximizing the value of IC_{50}

Models	Element Type	Values
Cytoplasm	Hyperelastic	D_1=1666.7MPa^{-1}, $\mu_0 = 2C_{10}$,C_{10}=6.21*10^5
Cell wall	Linear elastic	E=25 MPa, ν=0.16
Nano-pattern	Linear elastic	E=110000 MPa, ν=0.35

respectively. A visco-hyperelastic material (Neo-Hookean) was employed to model the cytoplasm of *E. coli.* Titanium is used for the nano-pattern. The main parameters used to analyze mechano-bactericidal are listed in Table 1 (Maleki *et al*. 2021).

The model has been meshed by a suitable three-dimensional element for an example of a tetrahedron element. The mesh discretization consists of 27310 elements and 51908 nodes (Fig. 3)

After defining all the data required for the element types, material properties, boundary conditions, and loadings, analyses were performed, and the example solution is given in Fig. 4.

2.2 Artificial neural network

Neural networks is a mathematical programming technique that mimics the functioning of the brain. ANNs can learn and classify complex processes, develop predictions, and make decisions (Asteris and Mokos 2020,

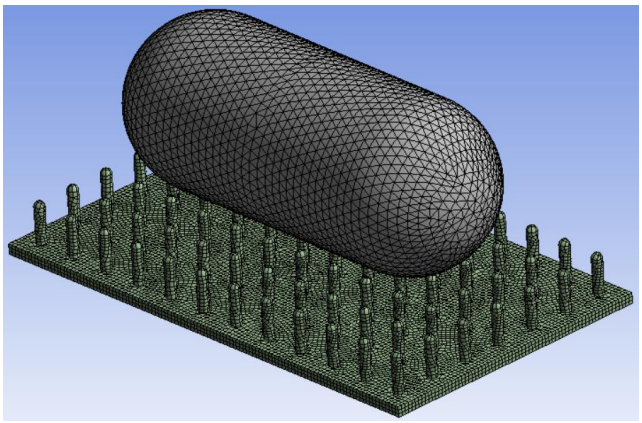

Fig. 3 Finite element mesh for the model

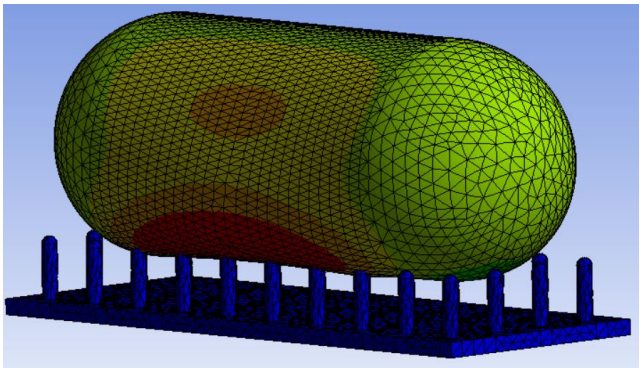

Fig. 4 Finite element model for mechano-bactericidal analysis

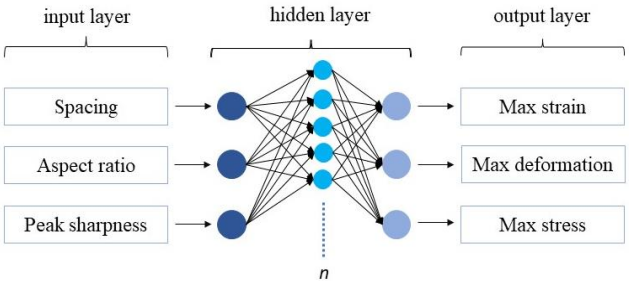

Fig. 5 The structure of the ANN

Table 2 Test parameters

Aspect ratio	Spacing	Peak sharpness
1	50	0
3	150	0.25
7	250	0.5
11	350	0.75
13	450	1
17	550	

Altabey *et al*. 2021, Uzun Yaylacı *et al*. 2020, 2022, Liu *et al*. 2022, Yaylacı *et al*. 2022c). ANNs comprise simple, organized, and interconnected processing units (Dawson and Wilby 1998). An artificial neural network consists of input, hidden, and output layers. The input layer collects the signals from the external environment. The hidden layer receives and processes information from the input layer. Finally, the output layer takes the weighted sum and produces the network output. The learning process in artificial neural networks occurs in two ways, supervised and unsupervised. Multilayer perceptron (MLP), with its simple structure, is the most used supervised learning approach (Yan *et al*. 2006). Fig. 5 shows the ANN structure.

With 148 values obtained from the FEM solutions, a database covering the entire data set and enabling the successful training of the network was created (Table 2). The input layer of the network consists of three neurons. These are as follows,

Spacing: Center-to-center distance

Aspect ratio: Height/width

Peak sharpness: Top of nanopillars

The output layer consisted of maximum strain, maximum deformation, and maximum stress.

The best network structure was determined by testing multiple architectures and considering the error rates of the networks. The number of neurons in the hidden layer affects the network's performance (Kavzoğlu 2001). An excessive or insufficient number of neurons may cause poor generalization or overfitting of ANN. The solution is trial and error (Le Cun *et al*. 1990). In this ANN model, a single hidden layer and 1 to 25 units were tested in this layer. The weights were randomly initialized between 0.0001 and 0.001. After comparing the appropriateness of the error functions (sum of squares and entropy), the activation functions (identity, logistic sigmoid, hyperbolic tangent, exponential, softmax, and Gaussian) were tested. In this study, the network was modeled with Broyden–Fletcher–Goldfarb–Shanno (BFGS), which is a numerical optimization algorithm that uses the second derivative (Hessian matrix) to calculate the change in parameter value at each iteration. Ten thousand networks were trained and retained for model structure. The ANN was performed using Statistica software 12. The program code was written in C++ to calculate the maximum strain, maximum deformation, and maximum stress.

3. Results and discussion

The deformation, stress, and strain analysis of the *E. coli* cell in contact with the nano-patterns surface was studied in a three-dimensional model using ANSYS based on FEM. The stress, strain, and deformation results of each analysis were obtained using ANSYS; result images are given below as an example (Fig. 6).

Validation Study: The accuracy of the FEM results was tested by comparing them with the study in the literature. The control of the conformity of the results was evaluated by considering the mean absolute error (e_{mae}). e_{mae} is used as the convenience equation to measure the productivity of the numerical results and is defined as (Mehar and Panda 2019),

$$e_{mae}=\left|\frac{R_{L_i}-R_{FEM_i}}{R_{L_i}}\right|\text{x}100,\quad e_{mae}=\left|\frac{R_{FEM_i}-R_{ANN_i}}{R_{FEM_i}}\right|\text{x}100\quad (i=1,2,3,...,n) \quad (1)$$

where R_{Li}, $R_{FEMi,}$ and R_{ANNi} are the literature, FEM, and

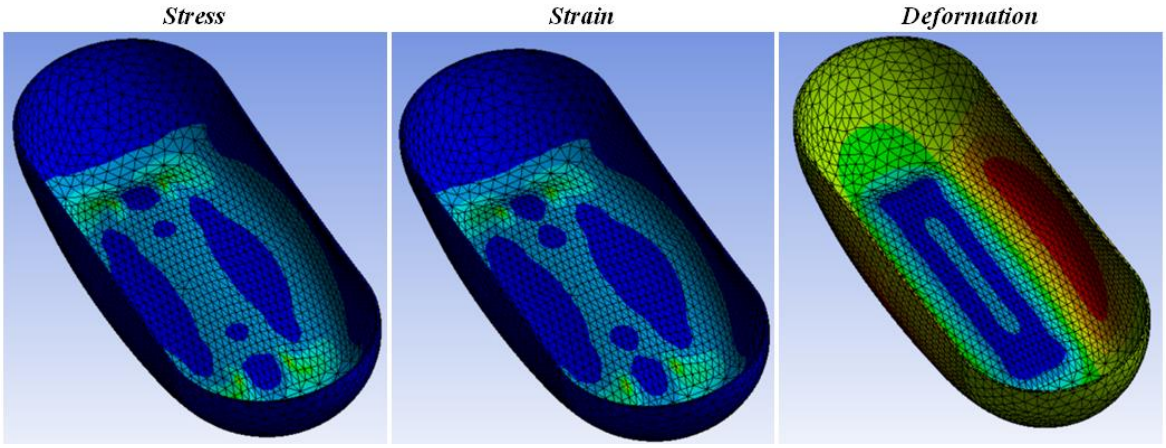

Fig. 6 Stress, strain, and deformation results of the model

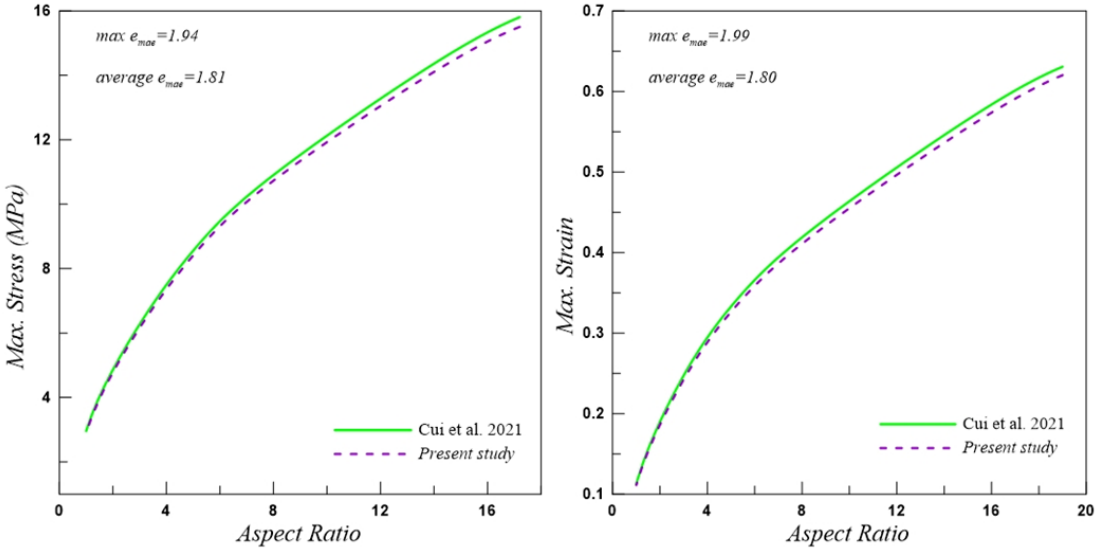

Fig. 7 Comparison of the max. stress and max. strain

ANN results, respectively. *n* denotes the total number of results.

Fig. 7 shows a comparative work for the stress and strain with the analytical results of Cui *et al.* (2021) to confirm the present method. The average and maximum errors of stress were calculated as e_{mae} = *1.94%* and e_{mae} = *1.81%*, respectively. The average and maximum errors of strain were calculated as e_{mae} = *1.99%* and e_{mae} = *1.80%*, respectively (Fig. 7). As seen from the figure, the current results obtained are in high agreement with the literature results. Furthermore, percentage error rates are very low and acceptable. Thus, it is concluded that the numerical solution approach made with this study is a good computational method for examining bacterial mechanics problems.

Fig. 8 shows that while the peak sharpness value is constant at 0.75, the increase in spacing and aspect ratio values increase the maximum strain, maximum deformation, and maximum stress on the *E. coli* cell wall. The fact that the increase in the aspect ratio calculated in this study can increase the bactericidal activity of the surfaces is similar to the report of Dickson *et al.* (2015).

In Fig. 9, while the spacing and aspect ratio values of nanopillars are constant, the effect of peak sharpness on maximum stress, maximum strain, and maximum deformation on the *E. coli* cell wall is presented. The pressure observed on the cell wall can be explained as the decrease in the peak sharpness value (1, the sharpest; 0, the shortest) increases the surface bactericidal efficiency when spacing is kept constant and the nanopillar height is sufficient.

Study 1: Fig. 10 shows the maximum stress, maximum strain, and maximum deformation with spacing considering the following dimensionless quantities: *(aspect ratio=4, peak sharpness=0.75*. It is seen that stress, strain, and deformation increase with the increase of the spacing. As can be seen in the figure, the maximum and average errors of maximum stress were calculated as *max* e_{mae} = *1.48%* and *average* e_{mae} = *1.19%*, respectively. The maximum and average errors of maximum strain were calculated as *max* e_{mae} = *1.97%* and *average* e_{mae} = *1.76%*, respectively. Finally, the maximum and average errors of maximum deformation were calculated as *max* e_{mae} = *1.85%* and *average* e_{mae} = *1.49%*, respectively.

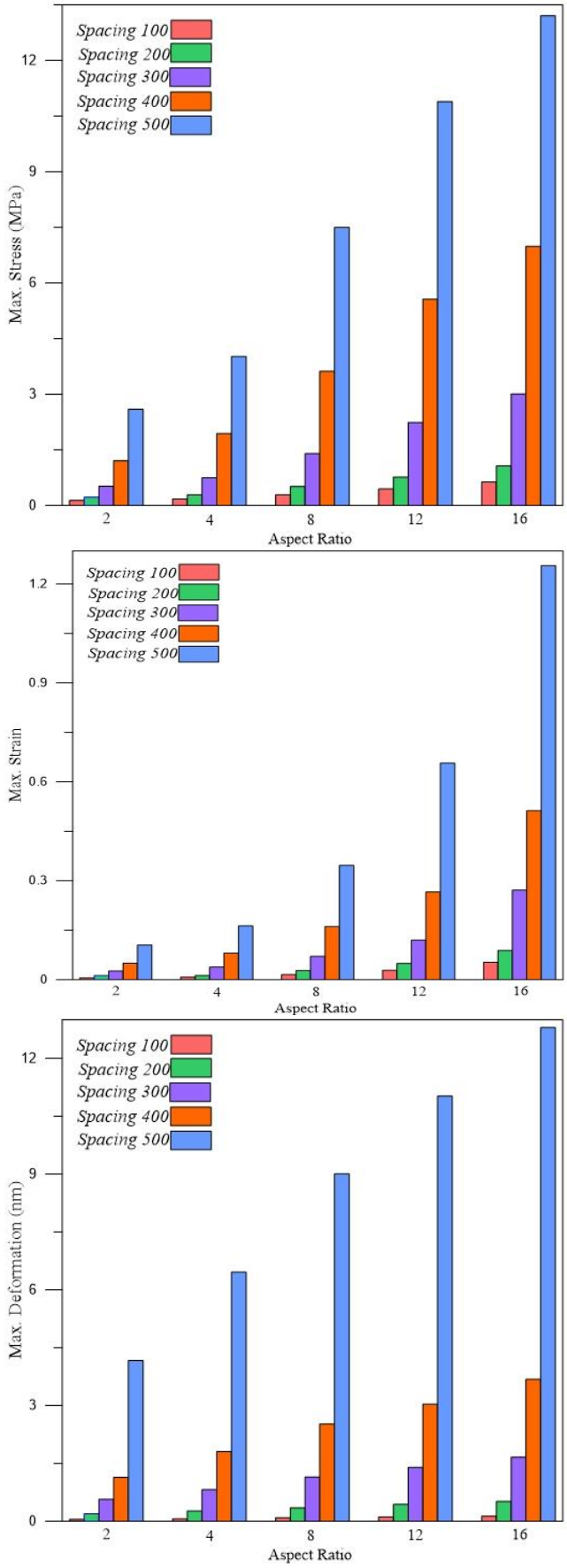

Fig. 8 The variation of the max. stress, max. strain, and max. deformation with spacing

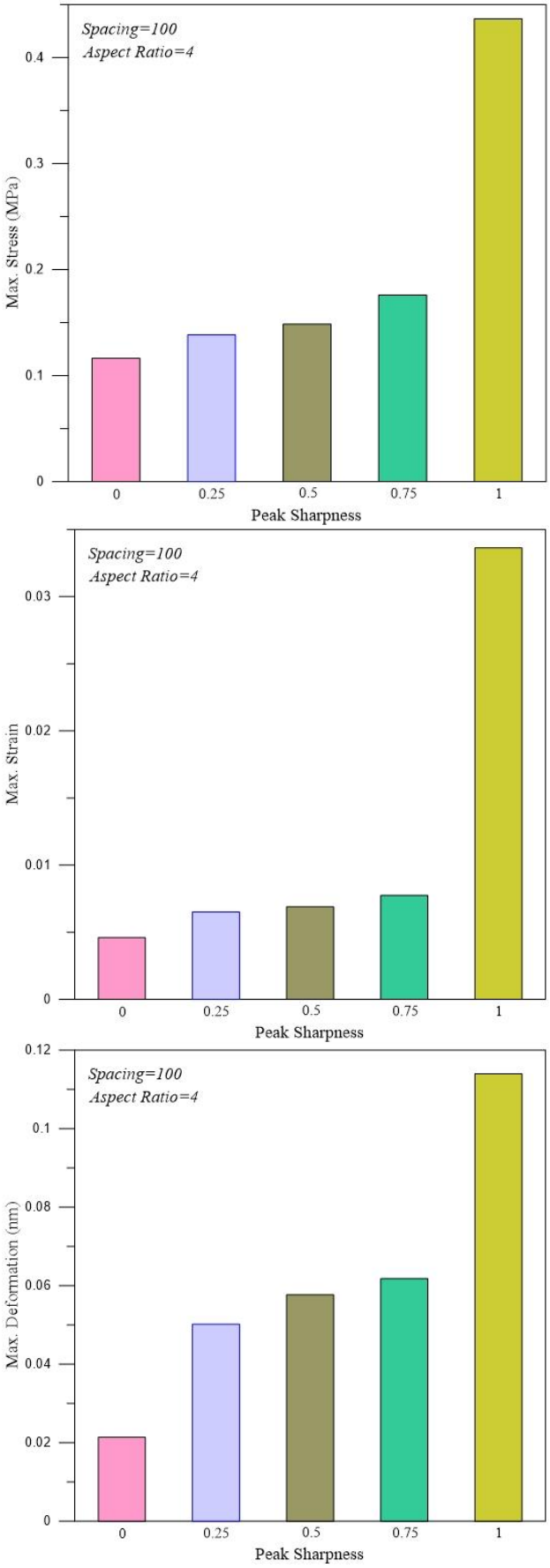

Fig. 9 The variation of the max. stress, max. strain and max. deformation with spacing

Table 3 The characteristic of the developed network model

Network	MLP	Learning error (%)	Testing error (%)	Validation error (%)	Learning algorithm	Error function	Hidden activation	Output activation
N_{MS}	3-19-1	1.11	0.09	0	BFGS 415	sos	Tanh	Exponential
N_{MD}	3-16-1	4.24	1.14	0	BFGS 603	sos	Tanh	Identity
N_{MST}	3-15-1	1.96	0.03	3.68	BFGS 385	sos	Tanh	Exponential

BFGS: Broyden fletcher goldfarb shanno algorithm, sos: Sum of square, Tanh: Hyperbolic tangent function, N_{MS}: Network of maximum strain, N_{MD}: Network of maximum deformation, N_{MST}: Network of maximum stress

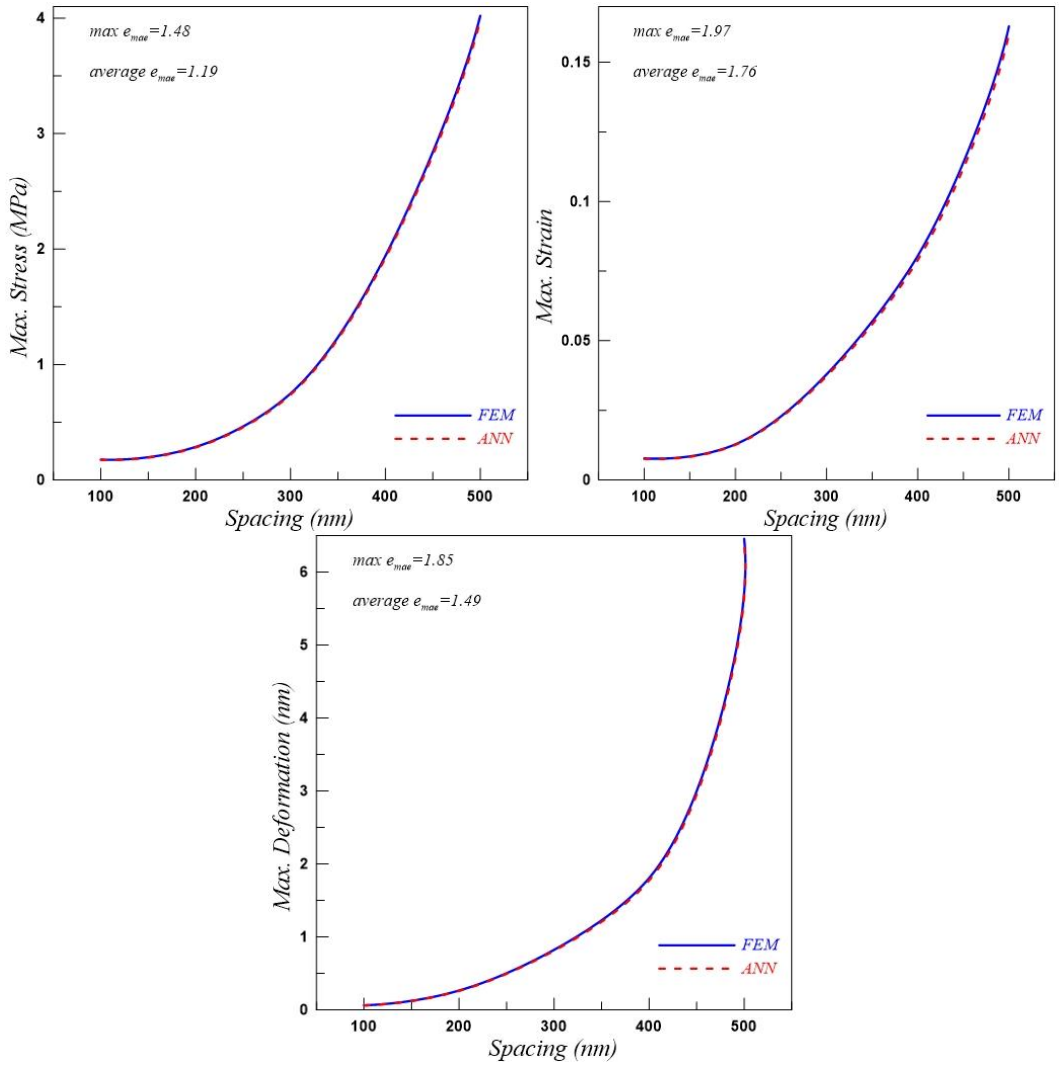

Fig. 10 The variation of the max. stress, max. strain and max. deformation with spacing

Study 4: Tables 4-6 show the comparisons of results of FEM and ANN methods for stress, strain, and deformation given in Figs. 10-12 using Root Mean Square Error (*RMSE*) and coefficient of determination (R^2). Checking the agreement of numerical results was evaluated by calculating RMSE and R^2. It was found that non-dimensional stress, strain, and deformation obtained from FEM and ANN agreed well.

A low obtained RMSE value indicates that the solutions are compatible. The closer this value is to zero, the closer the numerical solutions are to each other. R^2 is a statistical expression that numerically shows the relationship between FEM and ANN results. This value ranges from 0 to 1, and R^2>0.80 indicates a high correlation between FEM and ANN results. The RMSE and R^2 can be expressed as follows (Ren *et al*. 2022);

$$RMSE = \sqrt{\frac{1}{n}\sum_{i}^{n}\left(R_{FEM_i} - R_{ANN_i}\right)^2}, \quad (i = 1,2,3,...,n) \tag{2}$$

$$R^2 = 1 - \frac{\sum_{i}^{n}\left(R_{FEM_i} - R_{ANN_i}\right)^2}{\sum_{i}^{n}\left(R_{FEM_i} - \overline{R}_{FEM}\right)^2}, \quad (i = 1,2,3,...,n) \tag{3}$$

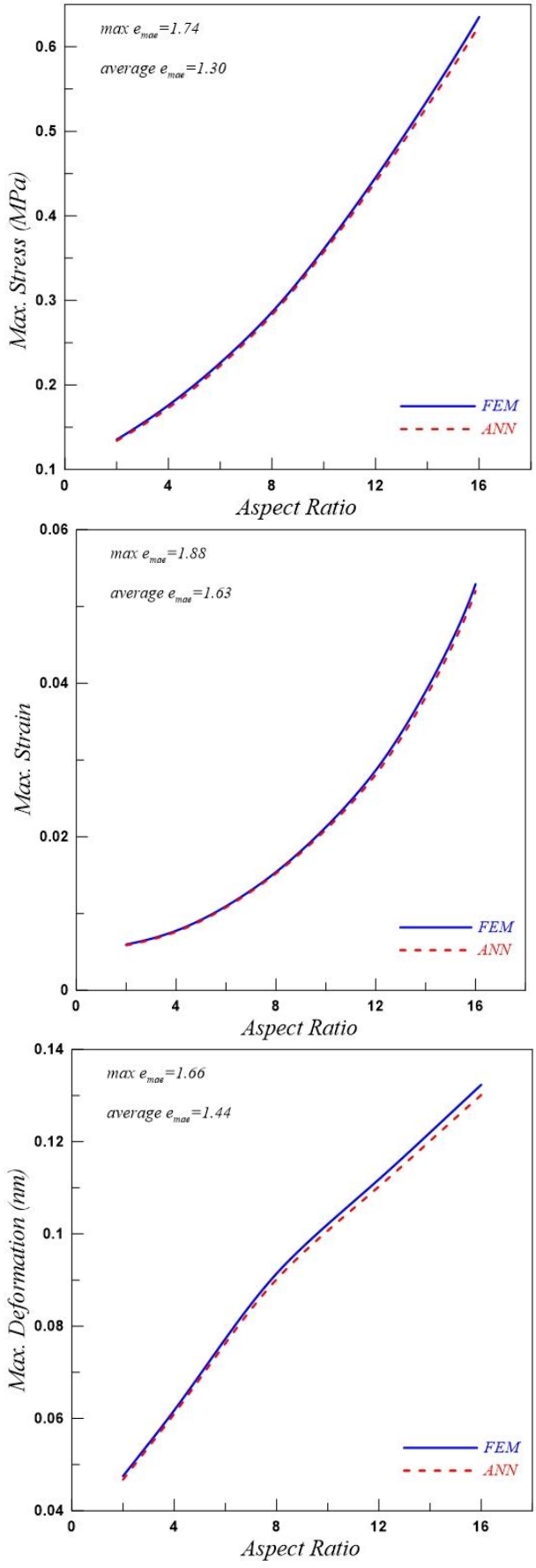

Fig. 11 The variation of the max. stress, max. strain and max. deformation with the aspect ratio

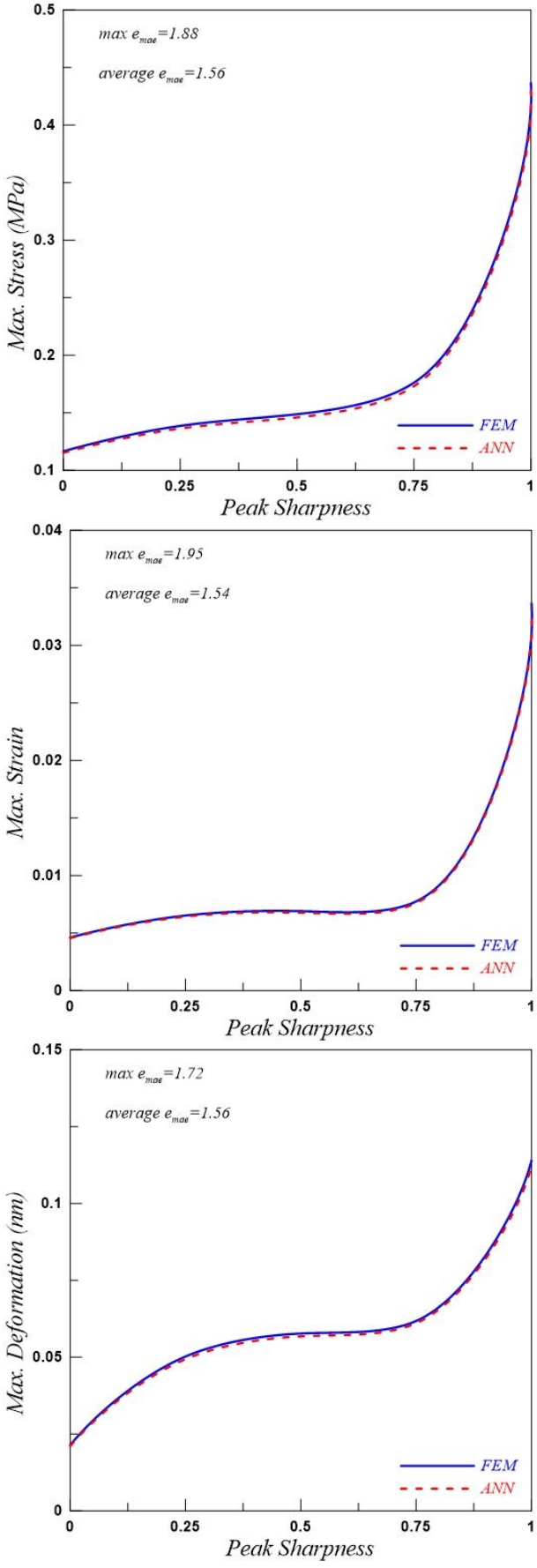

Fig. 12 The variation of the max. stress, max. strain and max. deformation with peak sharpness

Table 4 RMSE and R^2 for max. stress

Figure	Parameters	Max. Stress (MPa)	
		RMSE	R^2
Fig. 10	Spacing	0.0011	0.99995
	Aspect ratio	0.0029	0.99987
	Peak sharpness	0.0009	0.99999

Table 5 RMSE and R^2 for max. strain

Figure	Parameters	Max. Stress (MPa)	
		RMSE	R^2
Fig. 11	Spacing	0.0021	0.99988
	Aspect ratio	0.0019	0.99991
	Peak sharpness	0.0006	0.99999

Table 6 RMSE and R2 for max. deformation

Figure	Parameters	Max. Stress (MPa)	
		RMSE	R^2
Figure 12	Spacing	0.0035	0.99983
	Aspect ratio	0.0012	0.99998
	Peak sharpness	0.0007	0.99999

4. Conclusions

In this study, the mechano-bactericidal effect of geometric parameters such as peak sharpness, aspect ratio, and spacing of nanopillars was investigated by FEM. Elastic and creep deformation models of an *E. coli* cell adhered to the nanosurface were created. Cell deformation, stress, and strain were calculated. The results showed that the increase in peak sharpness, aspect ratio, and spacing values increased the maximum deformation, maximum stress, and maximum strain in the *E. coli* cell wall. In addition, the study observed that the results of the FEM and ANN methods were in good agreement with each other.

Nano-patterned surfaces show the potential to be used as a functional, environmentally friendly, and sustainable antibacterial material regarding non-toxicity and non-resistance in bacteria. Within the scope of this study, *in silico* investigation of the geometric structures of nano-patterned surfaces will assist in the design of more efficient mechano-bactericidal surfaces in the future.

References

Abharian, S., Sarfarazi, V., Marji, M.F., Rasekh, H. and Sadrekarimi, A. (2023), "Effect of geogrid reinforcement on tensile failure of high-strength self-compacted concrete", *Mag. Concr. Res.*, **75**(8), 379-401. https://doi.org/10.1680/jmacr.21.00284.

Alameda, M.T., Osorio, M.R., Pedraz, P. and Rodríguez, I. (2022), "Mechano-dynamic analysis of the bactericidal activity of bioinspired moth-eye nanopatterned surfaces", *Adv. Mater. Interf.*, **9**, 2270127. https://doi.org/10.1002/admi.202270127.

Altabey, W.A., Noori, M., Alarjani, A. and Zhao, Y. (2020), "Nano-delamination monitoring of BFRP nano-pipes of electrical potential change with ANNs", *Adv. Nano Res.*, **9**(1), 1-13. https://doi.org/10.12989/anr.2020.9.1.001.

ANSYS Mechanical APDL (2013), *ANSYS Contact Technology Guide*, Ansys Inc., Canonsburg, Pennsylvania, U.S.A.

Asteris, P.G. and Mokos, V.G. (2020), "Concrete compressive strength using artificial neural networks", *Neural. Comput. Appl.*, **32**, 11807-11826. https://doi.org/10.1007/s00521-019-04663-2.

Bagherifard, S., Hickey, D.J., de Luca, A.C., Malheiro, V.N., Markaki, A.E., Guagliano, M. and Webster, T.J. (2015), "The influence of nanostructured features on bacterial adhesion and bone cell functions on severely shot peened 316L stainless steel", *Biomaterials*, **73**, 185-197. https://doi.org/10.1016/j.biomaterials.2015.09.019.

Bouafia, H., Chikh, A., Bousahla, A.A., Bourada, F., Heireche, H., Tounsi, A., Benrahou, K.H., Tounsi, A., Al-Zahrani, M.M. and Hussain, M. (2021), "Natural frequencies of FGM nanoplates embedded in an elastic medium", *Adv. Nano Res.*, **11**(3), 239-249. https://doi.org/ 10.12989/anr.2021.11.3.239.

Cao, Y., Su, B., Chinnaraj, S., Jana, S., Bowen, L., Charlton, S., Duan, P., Jakubovics, N.S. and Chen, J. (2018), "Nanostructured titanium surfaces exhibit recalcitrance towards Staphylococcus epidermidis biofilm formation", *Sci. Rep.*, **8**, 1071. https://doi.org/10.1038/s41598-018-19484-x.

Cui, Q., Liu, T., Li, X., Zhao, L., Wu, Q.,Wang, X., Song, K. and Ge, D. (2021), "Validation of the mechano-bactericidal mechanism of nanostructured surfaces with finite element simulation", *Colloids Surf. B*, **206**, 111929. https://doi.org/10.1016/j.colsurfb.2021.111929.

DarAssi, M. and Hadji, L. (2014), "Analysis of the interplay between sedimentation and thermophoresis in the presence of convection in colloidal suspensions", *Proceedings of the ASME 2014 4th Joint US-European Fluids Engineering Division Summer Meeting*, **46247**, V01DT32A001 https://doi.org/10.1115/FEDSM2014-21078.

DarAssi, M. (2021), "Convective stability of CO2 sequestration in a porous medium", *Nonlinear Dyn. Syst. Theor.*, **21**(2), 179-192.

Dawson, C.W. and Wilby, R. (1998), "An artificial neural network approach to rainfall-runoff modelling", *Hydrolog. Sci. J.*, **43**(1), 47-66. https://doi.org/10.1080/02626669809492102.

Dickson, M.N., Liang, E.I., Rodriguez, L.A., Vollereaux, N. and Yee, A.F. (2015), "Nanopatterne polymer surfaces with bactericidal properties", *Biointerphases*, **10**(2), 021010. https://doi.org/10.1116/1.4922157.

Eltaher, M.A., Almalki, T.A., Ahmed, K.I.E. and Almitani, K.H. (2019), "Characterization and behaviors of single walled carbon nanotube by equivalent-continuum mechanics approach", *Adv. Nano Res.*, **7**(1), 39. https://doi.org/10.12989/anr.2019.7.1.039.

Fu, J., Haeri, H., Sarfarazi, V., Babanouri, N., Rezaei, A., Manesh, M.O., Bahrami, R. and Marji, M.F. (2023), "Effects of axial loading width and immediate roof thickness on the failure mechanism of a notched roof in room and pillar mining: experimental test and numerical simulation", *Rock Mech. Rock Eng.*, **56**, 719-745. https://doi.org/10.1007/s00603-022-03082-5.

Green, D.W., Lee, K.K.H., Watson, J.A., Kim, H.Y., Yoon, K.S., Kim, E.J., Lee, J.M., Watson, G.S. and Jung H.S. (2017), "High quality bioreplication of intricate nanostructures from a fragile gecko skin surface with bactericidal properties", *Sci. Rep.*, **7**, 41023. https://doi.org/10.1038/srep41023.

Hadji, L. and DarAssi, M. (2014), "Influence of sedimentation on the threshold for Soret-driven convection in colloidal suspensions", *Phys. Rev. E.*, **89**(1). https://10.1103/PhysRevE.89.013014.

Hazell, G., Fisher, L.E., Murray, W.A., Nobbs, A.H. and Su, B. (2018), "Bioinspired bactericidal surfaces with polymer nanocone arrays", *J. Colloid Interf. Sci.*, **528**, 389-399.

https://doi.org/10.1016/j.jcis.2018.05.096.

Ivanova, E.P., Hasan, J., Webb, H.K., Truong, V.K., Watson, G.S., Watson, J.A., Baulin, V.A., Pogodin, S., Wang, J.Y., Tobin, M.J., Löbbe, C. and Crawford, R.J. (2012), "Natural bactericidal surfaces: mechanical rupture of Pseudomonas aeruginosa cells by cicada wings", *Small (Weinheim an der Bergstrasse, Germany)*, **8**(16), 2489-2494. https://doi.org/10.1002/smll.201200528.

Ivanova, E.P., Linklater, D.P., Werner, M., Baulin, V.A., Xu, X., Vrancken, N., Rubanov, S., Hanssen, E., Wandiyanto, J., Truong, V.K., Elbourne, A., Maclaughlin, S., Juodkazis, S. and Crawford, R.J. (2020), "The multi-faceted mechano-bactericidal mechanism of nanostructured surfaces", *Proc. Natl. Acad. Sci. U.S.A.*, **117**(23), 12598-12605. https://doi.org/10.1073/pnas.1916680117.

Jiang, R., Hao, L., Song, L., Tian, L., Fan, Y., Zhao, J., Liu, C., Ming, W. and Ren, L. (2020), "Lotus-leaf-inspired hierarchical structured surface with non- fouling and mechanical bactericidal performances", *Chem. Eng. J.*, **398**, 125609. https://doi.org/10.1016/j.cej.2020.125609.

Kavzoglu, T. (2001), "An investigation of the design and use of feedforward artificial neural networks in the classification of remotely sensed images", Ph.D. Thesis, School of Geography, University of Nottingham.

Kumar, Y., Gupta, A. and Tounsi, A. (2021), "Size-dependent vibration response of porous graded nanostructure with FEM and nonlocal continuum model", *Adv. Nano Res.*, **11**(1), 1-17. https://doi.org/10.12989/anr.2021.11.1.001.

Le Cun, Y., Denker, J.S. and Solla, S.A., (1990), "Optimal brain damage", *Adv. Neural Infrom. Pr. Syst.*, **2**, 598-605.

Linklater, D.P., Juodkazis, S., Rubanov, S. and Ivanova, E.P. (2017), "Comment on "Bactericidal effects of natural nanotopography of dragonfly wing on Escherichia coli", *ACS Appl. Mater. Interf.*, **9**, 29387-29393. https://doi.org/10.1021/acsami.7b05707.

Liu, Q., Peng, K., Zeng, J., Marzouki, R., Majdi, A., Jan, A., Salameh, A.A. and Assilzadeh, H. (2022), "Effects of mining activities on Nano-soil management using artificial intelligence models of ANN and ELM", *Adv. Nano Res.*, **12**(6), 549-566. https://doi.org/10.12989/anr.2022.12.6.549.

Maleki, E., Mirzaali, M.J., Guagliano, M. and Bagherifard, S. (2021), "Analyzing the mechano-bactericidal effect of nano-patterned surfaces on different bacteria species", *Surf. Coat. Technol.*, **408,** 126782. https://doi.org/10.1016/j.surfcoat.2020.126782.

Meek R.W., Vyas, H. and Piddock, L.J.V. (2015), "Nonmedical uses of antibiotics: time to restrict their use?", *PLoS Biol.*, **13**(10), e1002266. https://doi.org/10.1371/journal.pbio.1002266.

Mehar, K. and Panda, S.K. (2019), "Multiscale modeling approach for thermal buckling analysis of nanocomposite curved structure", *Adv. Nano Res.*, **7(3),** 181-190. https://doi.org/10.12989/anr.2019.7.3.181.

Mirzaali, M.J., van Dongen, I.C.P., Tumer, N., Weinans, H., Yavari, S.A. and Zadpoor, A.A. (2018), "In-silico quest for bactericidal but non-cytotoxic nanopatterns", *Nanotechnology*, **29**, 43LT02. https://doi.org/10.1088/1361-6528/aad9bf.

Noori, M., Khanlari, G., Rafiei, B., Sarfarazi, V. and Zaheri, M. (2022), "Correction to: Estimation of brittleness indexes from petrographic characteristics of different sandstone types (cenozoic and mesozoic sandstones), Markazi Province, Iran", *Rock Mech. Rock Eng.*, **55**. https://doi.org/10.1007/s00603-022-02934-4.

Özdemir, M.E. and Yaylacı, M. (2023), "Research of the impact of material and flow properties on fluid-structure interaction in cage systems", *Wind. Struct. An Int. J.*, **36**(1), 31-40. https://doi.org/10.12989/was.2023.36.1.031.

Pandey, H.K., Hirwani, C.K., Sharma, N., Katariya, P.V. and Panda, S.K. (2019), "Effect of nano glass cenosphere filler on hybrid composite eigenfrequency responses - An FEM approach and experimental verification", *Adv. Nano Res.*, **7**(6), 419-429. https://doi.org/10.12989/anr.2019.7.6.419.

Pogodin, S., Hasan, J., Baulin, V.A., Webb, H.K., Truong, V.K., Phong Nguyen, T.H., Boshkovikj, V., Fluke, C. J., Watson, G.S., Watson, J.A., Crawford, R.J. and Ivanova, E.P. (2013), "Biophysical model of bacterial cell interactions with nanopatterned cicada wing surfaces", *Biophys. J.*, **104**(4), 835-840. https://doi.org/10.1016/j.bpj.2012.12.046.

Ren, W., Wu, X. and Cai, R. (2022), "A hybrid artificial intelligence and IOT for investigation dynamic modeling of nano-system", *Adv. Nano Res.*, **13**(2), 165-174. https://doi.org/10.12989/anr.2022.13.2.165.

Roy, A. and Chatterjee, K., (2021), "Theoretical and computational investigations into mechanobactericidal activity of nanostructures at the bacteria-biomaterial interface: a critical review", *Nanoscale*, **13**, 647. https://doi.org/10.1039/D0NR07976F.

Sun, T.C., DarAssi, M., Bilal, M. and Khan, M.A. (2022), "The study of Darcy-Forchheimer hybrid nanofluid flow with the thermal slip and dissipation effect using parametric continuation approach over a rotating disk", *Waves Random Complex Med.*, https://doi.org/10.1080/17455030.2022.2072537.

Turner, R.D., Hurd, A.F., Cadby, A., Hobbs, J.K. and Foster, S.J. (2013), "Cell wall elongation mode in Gram-negative bacteria is determined by peptidoglycan architecture", *Nat. Commun.*, **4,** 1496. https://doi.org/10.1038/ncomms2503.

Uzun Yaylacı, E. (2021), "Isolation and characterization of *Bacillus* spp. from aquaculture cage water and its inhibitory effect against selected *Vibrio* spp", *Arch. Microbiol.*, **204**(1), 26. https://doi.org/10.1007/s00203-021-02657-0.

Uzun Yaylacı, E., Öner, E., Yaylacı, M., Özdemir, M.E., Abushattal, A. and Birinci, A. (2022), "Application of artificial neural networks in the analysis of the continuous contact problem", *Struct. Eng. Mech.*, **84**(1), 35-48. https://doi.org/10.12989/sem.2022.84.1.035.

Uzun Yaylacı, E., Yaylacı, M., Ölmez, H. and Birinci, A. (2020), "Artificial neural network calculations for a receding contact problem", *Comput. Concr.*, **25**(6). https://doi.org/10.12989/cac.2020.25.6.551.

Vadillo-Rodriguez, V., Schooling, S.R. and Dutcher, J.R. (2009), "In situ characterization of differences in the viscoelastic response of individual gram-negative and gram-positive bacterial cells", *J. Bacteriol.*, **191**(17), 5518-5525. https://doi.org/10.1128/JB.00528-09.

Velic, A., Hasan, J., Li, Z. and Yarlagadda, P. (2021), "Mechanics of bacterial interaction and death on nanopatterned surfaces", *Biophys. J.*, **120**(2), 217-231. https://doi.org/10.1016/j.bpj.2020.12.003.

Yan, H., Jiang, Y., Zheng, J., Peng, C. and Li, Q. (2006), "A multilayer perceptron-based medical decision support system for heart disease diagnosis", *Expert Syst. Appl.*, **30**(2), 272-281. https://doi.org/10.1016/j.eswa.2005.07.022.

Yaylacı, M., Yaylı, M., Uzun Yaylacı, E., Ölmez, H. and Birinci, A. (2021), "Analyzing the contact problem of a functionally graded layer resting on an elastic half plane with theory of elasticity, finite element method and multilayer perceptron", *Struct. Eng. Mech.*, **78**(5), 585-597. https://doi.org/10.12989/sem.2021.78.5.585.

Yaylacı, M. (2022), "Simulate of edge and an internal crack problem and estimation of stress intensity factor through finite element method", *Adv. Nano Res.*, **12**(4), 405-414. https://doi.org/10.12989/anr.2022.12.4.405.

Yaylacı, M., Abanoz, M., Uzun Yaylacı, E., Ölmez, H., Sekban, M.D. and Birinci, A. (2022a), "The contact problem of the

functionally graded layer resting on rigid foundation pressed via rigid punch", *Steel Compos. Struct.*, **43**(5), 661-672. https://doi.org/10.12989/scs.2022.43.5.661.

Yaylacı, M., Şengül Şabano, B., Özdemir, M.E. and Birinci, A. (2022b), "Solving the contact problem of functionally graded layers resting on a homogeneous half-plane and pressed with a uniformly distributed load by analytical and numerical methods", *Struct. Eng. Mech.*, **82**(3), 401-416. https://doi.org/10.12989/sem.2022.82.3.401.

Yaylacı, M., Uzun Yaylacı, E., Özdemir, M.E., Ay, S., and Öztürk, Ş. (2022c), "Implementation of finite element and artificial neural network methods to analyze the contact problem of a functionally graded layer containing crack", *Steel Compos. Struct.*, **45**(4), 501-511. https://doi.org/10.12989/scs.2022.45.4.501.

Zhou, C., Koshani, R., O'Brien, B., Ronholm, J., Cao, X. and Wang, Y. (2021), "Bio-inspired mechano-bactericidal nano-structures: A promising strategy for eliminating surface foodborne bacteria", *Curr. Opin. Food Sci.*, **39**, 110-119. https://doi.org/10.1016/j.cofs.2020.12.021.

CC